Journal of Materials Chemistry

Cite this: J. Mater. Chem., 2012, 22, 14639

www.rsc.org/materials

PAPER

Effect of polymer chain conformation on field-effect transistor performance: synthesis and properties of two arylene imide based D–A copolymers†

Dugang Chen,[a] Yan Zhao,[b] Cheng Zhong,[a] Siqi Gao,[a] Gui Yu,[b] Yunqi Liu*[b] and Jingui Qin*[a]

Received 21st March 2012, Accepted 10th May 2012
DOI: 10.1039/c2jm31755a

Two donor–acceptor (D–A) alternating copolymers (**P1** and **P2**) with phthalimide or thieno[3,4-*c*]pyrrole-4,6-dione as the electron acceptor and bithiophene as the electron donor have been synthesized by Stille polycondensation. Both polymers showed good thermal stability and a low HOMO level. Organic field-effect transistor (OFET) devices with common architectures were fabricated to evaluate and compare the FET properties of the two polymers. Though **P2** exhibits better coplanarity than **P1**, the FET results revealed that both the hole mobility and current on–off ratio of **P1** are more than one order of magnitude higher than **P2**. Theoretical calculations and AFM were conducted to analyze the reason for this very interesting result, and it was found that polymer chain conformation is another important factor (in addition to coplanarity) for polymers to obtain high FET performance.

Introduction

Over the past decade, conjugated polymers have attracted intense interest for their potential applications in optoelectronic devices such as organic light-emitting diodes (OLEDs), organic photovoltaic cells (OPVs) and organic field-effect transistors (OFETs).[1–4] They showed great advantages with diverse structures, tunable properties and good solution processability, which permit a low-cost fabrication process for producing compact, light-weight and flexible electronic devices.[5–7]

Significant progress has been achieved with polymer-based OFETs in recent years. Two main types of polymer have been designed as channel semiconductors with good FET performance in this area. One is polymers with an electron-rich main chain and ordered linear alkyl side chains, mostly constructed from thiophene derivatives, such as P3HT,[8,9] PQT-12[10,11] and PBTTT,[12] that can be well aligned when processed from solution to give a high mobility above 0.1 $cm^2 V^{-1} s^{-1}$. Nonetheless, their air stability must still be improved for practical applications. The other is the donor–acceptor (D–A) type of polymer with a main chain constructed by alternate electron-rich and -deficient moieties, which could more easily produce a low HOMO (highest occupied molecular orbital) level and lead to higher air stability than polymers constructed by electron-rich main chains. Some acceptor units derived from 2,1,3-benzothiadiazole (BT),[13,14] 3,6-diaryl-2,5-dihydropyrrolo[3,4-*c*]pyrrole-1,4-dione (DPP),[15–19] isoindigo,[20] thiazolothiazole,[21,22] and thienopyrazine (TP)[23,24] moieties, when conjugated with various electron-donating units, such as bithiophene, thieno[3,2-*b*]thiophene (TT), cyclopentadithiophene (CDT), and indacenodithiophene (IDT), have demonstrated distinguished FET performance with mobitilies up to 1.95 $cm^2 V^{-1} s^{-1}$.[25]

The electron-deficient arylene imide groups usually exhibit symmetric, rigid fused, coplanar structures and electron-withdrawing properties, which make them potential systems for increasing intermolecular interactions and lowering HOMO energy levels when incorporated into polymeric backbones,[26–30] leading to high hole mobility and good air stability. Therefore, we designed and prepared two new D–A copolymers based on arylene imide groups for OFETs. As shown in Fig. 1, phthalimide and thieno[3,4-*c*]pyrrole-4,6-dione were selected as acceptors for **P1** and **P2**, respectively. 2,2-bithiophene without any alkyl side chains was used as a donor that can ensure less steric hindrance from the adjacent acceptors or between themselves, and which may bring about an ordered molecular arrangement in thin films. The main chain of **P2** is constructed by five-membered thiophene rings, which should show better coplanarity than **P1**. In addition, to guarantee the solution processability of the polymers, a branched alkyl chain, 2-octyldodecyl, was attached to both acceptors. The synthesis and characterization of the two polymers are reported here, and the FET performances are evaluated using devices with bottom-contact/bottom-gate configuration. The structure–property relationships are analyzed and discussed with theoretical calculations and AFM measurements.

[a]*Department of Chemistry, Hubei Key Lab on Organic and Polymeric Optoelectronic Materials, Wuhan University, Wuhan 430072, China. E-mail: jgqin@whu.edu.cn; Tel: +86-27-68752330*
[b]*Beijing National Laboratory for Molecular Sciences, Institute of Chemistry, Chinese Academy of Sciences, Beijing 100190, China. E-mail: liuyq@iccas.ac.cn; Tel: +86-10-62613253*

† Electronic supplementary information (ESI) available: The synthesis of intermediates and monomers, and detailed theoretical calculation results for **P1** and **P2**. See DOI: 10.1039/c2jm31755a

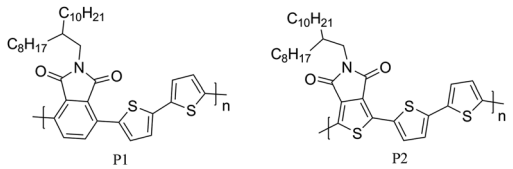

Fig. 1 The molecular structures of **P1** and **P2**.

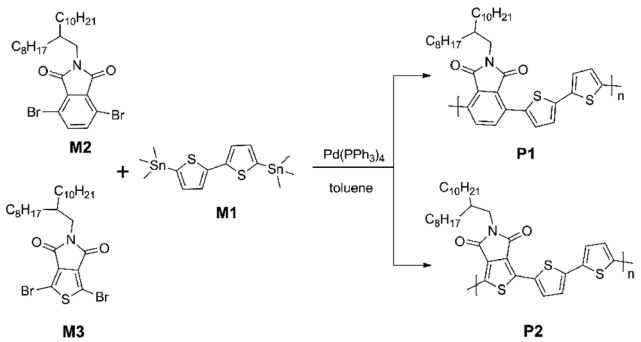

Scheme 1 The synthetic routes of the polymers.

Table 1 Molecular weights and thermal properties of the polymers

	M_n[a] (g mol^{-1})	M_w[a] (g mol^{-1})	PDIs[a]	T_d[b] (°C)
P1	1.17×10^4	2.94×10^4	2.51	442
P2	1.88×10^4	5.44×10^4	2.89	430

[a] Number-average molecular weight (M_n), weight-average molecular weight (M_w), and polydispersity indices (PDIs, M_w/M_n) determined by means of GPC with THF as eluent on the basis of polystyrene calibration. [b] Temperature at 5% weight loss estimated using TGA under N_2.

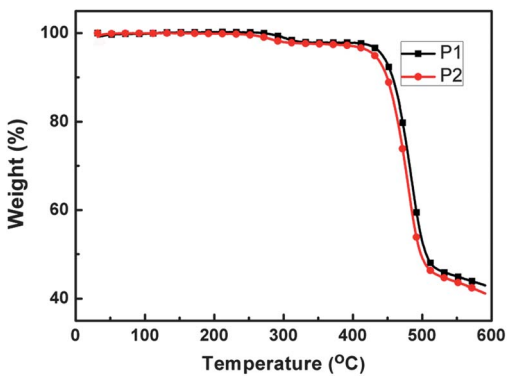

Fig. 2 TGA plots of the polymers.

Experimental

General information

^{1}H NMR and ^{13}C NMR spectra were measured on a MERCURY-VX300 spectrometer. Elemental analysis of carbon, hydrogen, and nitrogen was performed on a Vario EL III microanalyzer. UV-vis absorption spectra were recorded on a Shimadzu UV-2500 recording spectrophotometer. Gel permeation chromatography (GPC) analysis was performed on an Agilent 1100 series HPLC system equipped with a G1326A refractive index detector, in which polystyrene standards were used as the calibration standards and THF was used as the eluent, and the flow rate was 1.0 mL min^{-1}. Thermogravimetric analysis (TGA) was undertaken with a NETZSCH STA 449C instrument. The thermal stability of the samples under a nitrogen atmosphere was determined by measuring their weight loss while heating at a rate of 10 °C min^{-1}. Differential scanning calorimetry (DSC) was performed on a Mettler Toledo DSC822e unit at a heating rate of 10 °C min^{-1} from room temperature to 260 °C under nitrogen. Cyclic voltammetry (CV) was carried out in a nitrogen purged anhydrous CH_3CN solution at room temperature with a CHI voltammetric analyzer. Tetrabutylammonium hexafluorophosphate ($TBAPF_6$) (0.1 M) was used as the supporting electrolyte. The conventional three-electrode configuration consisted of a platinum working electrode, a platinum wire auxiliary electrode, and an Ag wire pseudo-reference electrode with ferrocenium–ferrocene (Fc^+–Fc) as the internal standard. Cyclic voltammograms were obtained at a scan rate of 100 mV s^{-1}. Formal potentials were calculated as the average of the cyclic voltammetric anodic and cathodic peaks. The onset potential was determined from the intersection of two tangents drawn at the rising and background current of the cyclic voltammogram. Atomic force microscopy (AFM) images were obtained on a Nanoscope V AFM (Digital Instruments) in tapping mode.

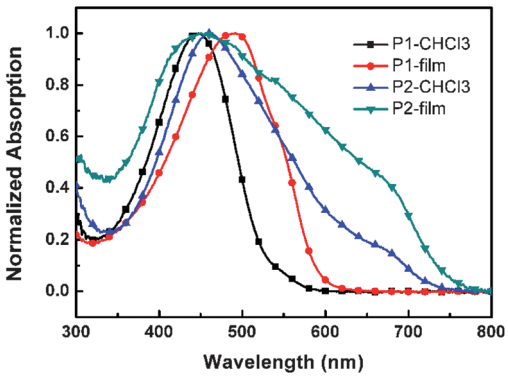

Fig. 3 UV-vis spectra of the polymers in chloroform and thin films.

Device fabrication and characterization

FET devices were fabricated with a bottom-contact/bottom-gate configuration. A heavily doped n-type Si wafer with a SiO_2 layer of 300 nm and a capacitance of 11 nF cm^{-2} was used as the gate dielectric. Octadecyltrichlorosilane (OTS) was used as a self-assembled surface modifier for SiO_2. The Au source–drain electrodes were prepared by photolithography. For the spin-coated thin film device, a 50 nm-thick (±10 nm) semiconductor film was spin-coated on top of the OTS-treated SiO_2 from a 10 mg mL^{-1} $CHCl_3$ solution of the polymers. The channel length was 5 μm, and the channel width was 1400 μm. Device annealing was carried out at 120 °C for 1 h in a vacuum oven under a pressure of 0.1 Pa. The current–voltage (I–V) characteristics were measured with the Micromanipulator 6150 probe station in a clean and metallic shielded box at room temperature in air, and recorded

Table 2 Optical and electrochemical data of the polymers

	Solution		Film			CV		
	λ_{max}[a] (nm)	λ_{onset}[b] (nm)	λ_{max}[a] (nm)	λ_{onset}[b] (nm)	E_g^{opt}[c] (eV)	HOMO[d] (eV)	LUMO[d] (eV)	E_g^{cve}[e] (eV)
P1	447	529	492	591	2.10	−5.42	−2.98	2.44
P2	460	729	456	751	1.65	−5.43	−3.09	2.34

[a] Absorption maxima. [b] The onset edge absorption. [c] Estimated from the onset edge of absorption in films: $E_g^{opt} = 1240/\lambda_{onset}$. [d] Estimated from the onset oxidation and reduction potentials, respectively, assuming the absolute energy level of ferrocene–ferrocenium to be 4.8 eV below vacuum. [e] HOMO–LUMO gap estimated from electrochemistry.

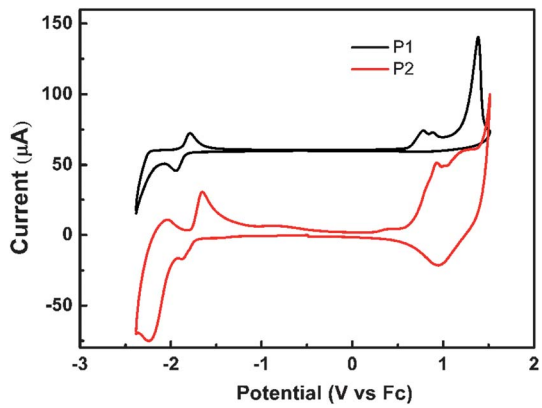

Fig. 4 The cyclic voltammograms of **P1** and **P2** films on a platinum electrode measured in 0.1 mol L^{-1} Bu_4NPF_6 acetonitrile solutions at a scan rate of 100 mV s^{-1}.

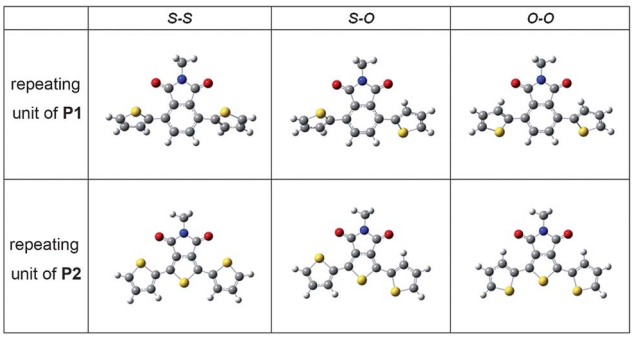

Fig. 6 Three possible conformers of the repeating units in **P1** and **P2**.

with a Keithley 4200 SCS. The field-effect mobility was calculated in the saturation regime by using the equation $I_{DS} = (\mu WC_i/2L)(V_G - V_T)^2$,[31] where I_{DS} is the drain–source current,

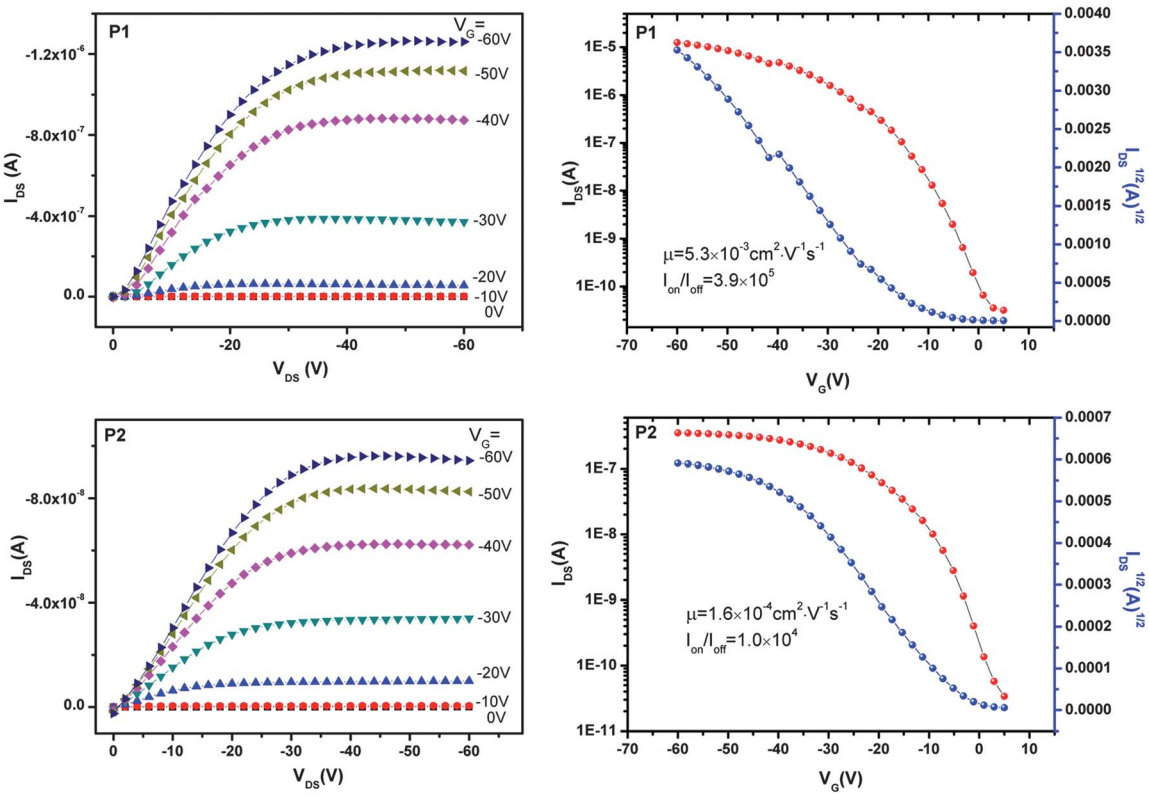

Fig. 5 Output characteristics at different gate bias (left) and transfer characteristics at constant source–drain voltage, $V_{DS} = -60$ V (right) for devices using **P1** and **P2** as semiconductors when annealed at 120 °C in vacuum.

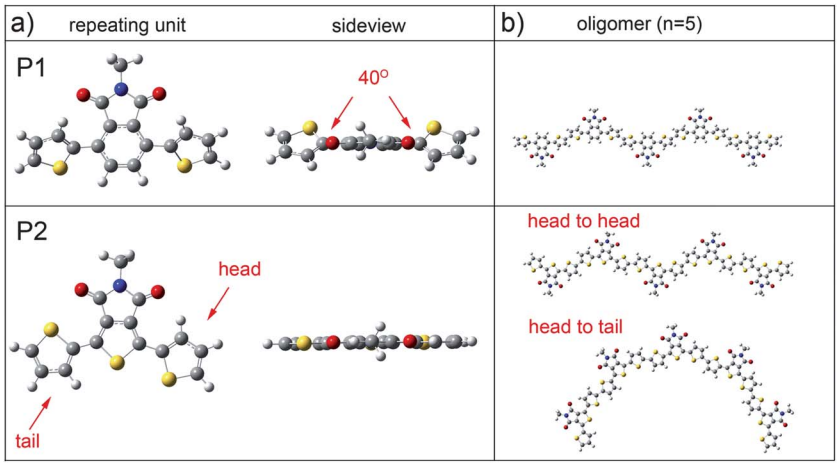

Fig. 7 (a) The preferred conformations of the repeating units and (b) the main chain conformations of oligomers in **P1** and **P2**.

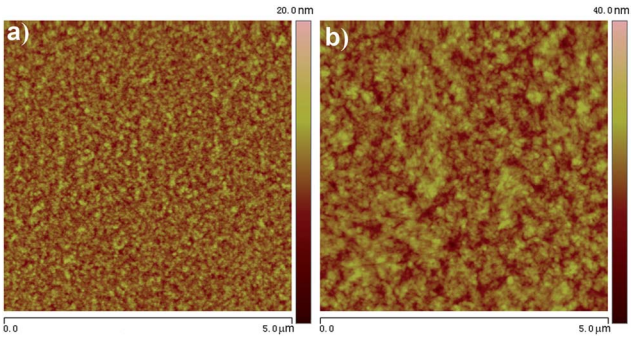

Fig. 8 AFM height images of spin-coated (a) **P1** and (b) **P2** films on OTS-modified SiO_2 substrate after annealing at 120 °C.

μ is the field-effect mobility, W is the channel width, L is the channel length, C_i is the capacitance per unit area of the gate dielectric layer, V_G is the gate voltage, and V_T is the threshold voltage.

Synthesis of polymers

Synthesis of P1. 4,7-dibromo-2-(2-octyldodecyl)isoindoline-1,3-dione (**M2**, 0.2096 g, 0.3580 mmol), 5,5′-bis(trimethylstannyl)-2,2′-bithiophene (**M1**, 0.1761 g, 0.3580 mmol) and $Pd(PPh_3)_4$ (17 mg, 2 mol%) were added to a Schlenk tube, which was then connected to a vacuum line and filled with argon. 10 mL of toluene was injected to the reactor using a syringe and the solution was warmed to 110 °C and stirred for 48 hours. After cooling to room temperature, the solution was poured into 200 mL of methanol. The precipitate was collected by filtration, and then extracted *via* a Soxhlet apparatus with methanol, acetone, hexane, and finally chloroform. Only the chloroform-soluble portion was collected, concentrated, and precipitated from methanol to give **P1** as a dark red solid. Yield: 0.16 g, 78%. ^{1}H NMR ($CDCl_3$, 300 MHz) δ [ppm]: 7.82 (br, 6H), 3.60 (br, 2H), 1.92 (br, 1H), 1.25 (br, 32H), 0.87 (br, 6H).

Synthesis of P2. The synthetic procedures were almost the same as that of **P1**, except that 1,3-dibromo-5-(2-octyldodecyl)-4H-thieno[3,4-c]pyrrole-4,6(5H)-dione (**M3**, 0.2099 g, 0.3549 mmol), **M1** (0.1745 g, 0.3548 mmol) and $Pd(PPh_3)_4$ (17 mg, 2 mol %) were used as the reactants. After the extraction, **P2** was obtained as a black solid. Yield: 0.17 g, 82%. ^{1}H NMR ($CDCl_3$, 300 MHz) δ [ppm]: 7.71 (br, 4H), 3.56 (br, 2H), 1.53–1.25 (m, 33H), 1.00 (br, 3H), 0.87 (br, 3H).

Results and discussion

Polymer synthesis and characterization

The three monomers were synthesized according to literature procedures (see ESI†).[32–35] **P1** and **P2** were obtained by the Stille coupling reaction in good yields as shown in Scheme 1. The polymers were purified by multiple Soxhlet extractions to give the final products as dark red and black solids, respectively. Both of them showed good solubility in some organic solvents, such as chloroform, chlorobenzene, toluene and THF. This solubility satisfies a significant requirement for the fabrication of semiconductors. Molecular weights and polydispersity indices (PDIs) of the polymers, as shown in Table 1, were determined by gel permeation chromatography (GPC) in THF using a polystyrene standard as the calibrant.

Thermal properties

The thermal properties of the polymers were evaluated by TGA and DSC under nitrogen. As shown in Fig. 2, the decomposition temperature (T_d) at 5% weight loss for **P1** and **P2** are both above 430 °C, which is high enough for device fabrication. In addition, the thermograms showed that a slight weight loss started at 270 °C for both polymers, which is attributed to the release of captured solvent molecules activated by the polymer chains' thermal movements.[36] However, the DSC results did not provide any information on glass transition temperatures for the polymers in the range of our study.

Optical properties

The normalized UV-vis absorption spectra of **P1** and **P2** were measured in chloroform (*ca.* 10^{-5} M) and in thin films spin-coated on a quartz substrate (Fig. 3), and the results are

summarized in Table 2. The absorption maximum of **P1** in film showed a large red-shift of about 45 nm relative to that in solution, indicating that the molecules could be well arranged and aggregate in solid states owing to the strong interchain interactions, which may facilitate charge transport. However, this phenomenon didn't appear in the absorption of **P2**. The absorption maxima of **P2** were almost the same, at about 460 nm, either in film or in solution. The optical band gaps of **P1** and **P2**, estimated from the onset of absorption in the solid films, were 2.10 and 1.65 eV, respectively.

Electrochemical properties

The redox behaviors for **P1** and **P2** were investigated by cyclic voltammetry. Fig. 4 shows the cyclic voltammograms of two polymer films on a Pt disk electrode in 0.1 mol L^{-1} Bu_4NPF_6 acetonitrile solution. As shown in the figure, both **P1** and **P2** showed similar behavior in the negative potential region, while in the positive potential region, **P1** demonstrates an irreversible oxidation/re-reduction process while **P2** demonstrates a reversible process. This small difference may come from the fact that they contain a different acceptor. The highest occupied molecular orbital (HOMO) and lowest unoccupied molecular orbital (LUMO) energy levels were estimated from the onset oxidation and reduction potentials, assuming the absolute energy level of ferrocene–ferrocenium is 4.8 eV below vacuum,[37–39] and the data is summarized in Table 2. Both polymers showed a low HOMO level of about −5.4 eV, indicating that the materials are not susceptible to oxidative doping, which is advantageous when the materials are applied to OFETs. The energy band gaps for **P1** and **P2** were 2.44 eV and 2.34 eV, respectively, significantly larger than their optical band gaps. This discrepancy might have been caused by the presence of an energy barrier at the interface between the polymer films and the electrode surface.

FET properties

The field-effect transistor performances of **P1** and **P2** were investigated by fabricating OFETs with the most basic architecture: bottom contact, bottom gate, and OTS-modified SiO_2 dielectric. Devices were annealed at 120 °C under vacuum and tested in ambient air conditions without any special precautions. Fig. 5 shows the typical output and transfer curves of the OFETs using **P1** and **P2** as the p-channel semiconductors. The output behaviors of both polymers followed closely the gradual-channel model employed in metal oxide semiconductor FETs with good saturation and ohmic contact. The threshold voltages of **P1** and **P2** based devices were −13.7 and 1.45 V, respectively. The mobility estimated at the saturated regime for the **P1** device was 5.3×10^{-3} cm^2 V^{-1} s^{-1} with a current on–off ratio of 3.9×10^5, and it was 1.6×10^{-4} cm^2 V^{-1} s^{-1} with a current on–off ratio of 1.0×10^4 for the **P2** device. It was surprising to notice that **P2** showed a hole mobility and current on–off ratio that were both more than one order of magnitude lower than for **P1**, although it was designed to give better coplanarity and expected to demonstrate better charge transport ability. Even when the effect of the molecular weight was considered, the result was still beyond expectations, because the higher molecular weight of **P2** did not show any mobility advantages over **P1**. To find out the reason for this, theoretical calculations and AFM analysis were performed to investigate the polymer structures and film morphology as follows.

Theoretical calculations

The thiophene rings (in the bithiophene unit) and the acceptor unit are connected by single bonds. So the sulfur atom of the thiophene ring and the nitrogen atom of the imide group can be on the same side (defined as *S* here) or on the opposite side (defined as *O* here). As a result, for each repeating unit in **P1** and **P2** there exists three conformers, namely, *S*–*S*, *S*–*O*, and *O*–*O* (Fig. 6). The geometries of these conformers were optimized at wb97xd/6-311g(d,p) level[40,41] and followed by a frequency calculation, then the Gibbs free energy were compared in order to figure out which conformer is more stable (see ESI†). Note that the calculations were performed on model systems of polymers where all alkyl chain substituents were replaced with methyl groups (this has only a minimal effect on the electronic properties).

Fig. 7a shows the preferred conformations of the repeating units in **P1** and **P2**. The stable conformation of the repeating unit in **P1** is *O*–*O*, and the dihedral angles between the thiophene ring and central acceptor are about 40°. Since two sulfur atoms in the bithiophene units are on the opposite side when the repeating unit is connected to form a polymer, the repeating unit of **P1** can join together to make up an ordered linear main chain (Fig. 7b). On the other hand, the repeating unit of **P2** shows much better coplanarity than that of **P1** as there is almost no torsion angle between the thiophene and the central acceptor unit. However, the stable conformation of the repeating unit in **P2** is *S*–*O*. Therefore, two kinds of connecting mode would appear when the repeating unit is connected to construct polymer **P2**, namely, head to tail or head to head connections (here we define *S* as the tail and *O* as the head of this conformer). Fig. 7b shows the two limited conformations of **P2** with arc-shaped and linear polymer chain, respectively. But in fact, the **P2** chains are made up by a two connecting mode randomly so that the whole chain conformation would be disorderly and cannot be confirmed. The uncertainty of the polymer chain conformation of **P2** may be harmful to the effective interchain π–π stacking in solid states, and hence lead to a lower mobility than that of **P1** in which the linear chains are easier to form π–π stacking though the coplanarity is not as good as in **P2**. This is also verified by the UV-vis absorption spectra as the absorption maximum of **P2** is not red-shifted from solution to thin films.

AFM analysis

The film morphology of the polymers was examined using AFM. Fig. 8 shows the tapping-mode AFM height images of spin-coated **P1** and **P2** films on OTS-modified SiO_2 substrate after annealing at 120 °C. Both polymer films show obvious crystalline grains on the surface, however, the grain size of **P2** is larger and the boundary is deeper than those of **P1**, which is not advantageous for charge transport between the grains. As a result, it's reasonable that the FET performance of **P2** device was lower than the **P1** device, which agrees with the results from theoretical calculations.

Conclusion

We have successfully synthesized two D–A copolymers containing phthalimide or thieno[3,4-*c*]pyrrole-4,6-dione as the acceptors. Both polymers showed good solubility, high thermal stability and a low HOMO level. The OFET measurements revealed that **P1** showed a hole mobility and current on–off ratio that were both more than one order of magnitude higher than **P2**, although the latter was designed to have better coplanarity than **P1**. Theoretical calculations were performed to simulate the structures of the repeating units and oligomers, and results revealed that **P2** indeed demonstrated better coplanarity, however, disordered main chain conformations were found to exist in **P2** which may be harmful to the interchain π–π stacking of the polymers and lead to a lower mobility. AFM analysis also verified that the thin film morphology of **P1** was more advantageous for charge transport than **P2**. In summary, this work demonstrates that the polymer chain conformation is another important factor (in addition to coplanarity) for polymers to show high FET performance.

Acknowledgements

This work was financially supported by the National Science Foundation of China.

Notes and references

1 C. Zhong, C. Duan, F. Huang, H. Wu and Y. Cao, *Chem. Mater.*, 2011, **23**, 326–340.
2 P. T. Boudreault, A. Najari and M. Leclerc, *Chem. Mater.*, 2011, **23**, 456–469.
3 I. McCulloch, M. Heeney, M. L. Chabinyc, D. DeLongchamp, R. J. Kline, M. Cölle, W. Duffy, D. Fischer, D. Gundlach, B. Hamadani, R. Hamilton, L. Richter, A. Salleo, M. Shkunov, D. Sparrowe, S. Tierney and W. Zhang, *Adv. Mater.*, 2009, **21**, 1091–1109.
4 L. Zhang, C. Di, G. Yu and Y. Liu, *J. Mater. Chem.*, 2010, **20**, 7059–7073.
5 F. Garnier, R. Hajlaoui, A. Yassar and P. Srivastava, *Science*, 1994, **265**, 1684–1686.
6 J. Liu, R. Zhang, I. Osaka, S. Mishra, A. E. Javier, D. Smilgies, T. Kowalewski and R. D. McCullough, *Adv. Funct. Mater.*, 2009, **19**, 3427–3434.
7 P. T. Boudreault, S. Wakim, M. L. Tang, Y. Tao, Z. Bao and M. Leclerc, *J. Mater. Chem.*, 2009, **19**, 2921–2928.
8 H. Sirringhaus, P. J. Brown, R. H. Friend, M. M. Nielsen, K. Bechgaard, B. M. W. Langeveld-Voss, A. J. H. Spiering, R. A. J. Janssen, E. W. Meijer, P. Herwig and D. M. de Leeuw, *Nature*, 1999, **401**, 685–688.
9 Z. Bao, A. Dodabalapur and A. J. Lovinger, *Appl. Phys. Lett.*, 1996, **69**, 4108–4110.
10 B. S. Ong, Y. Wu, P. Liu and S. Gardner, *J. Am. Chem. Soc.*, 2004, **126**, 3378–3379.
11 B. S. Ong, Y. Wu, P. Liu and S. Gardner, *Adv. Mater.*, 2005, **17**, 1141–1144.
12 I. McCulloch, M. Heeney, C. Bailey, K. Genevicius, I. Macdonald, M. Shkunov, D. Sparrowe, S. Tierney, R. Wagner, W. Zhang, M. L. Chabinyc, R. J. Kline, M. D. Mcgehee and M. F. Toney, *Nat. Mater.*, 2006, **5**, 328–333.
13 M. Zhang, H. N. Tsao, W. Pisula, C. Yang, A. K. Mishra and K. Müllen, *J. Am. Chem. Soc.*, 2007, **129**, 3473.
14 W. Zhang, J. Smith, S. E. Watkins, R. Gysel, M. McGehee, A. Salleo, J. Kirkpatrick, S. Ashraf, T. Anthopoulos, M. Heeney and I. McCulloch, *J. Am. Chem. Soc.*, 2010, **132**, 11437–11439.
15 J. C. Bijleveld, A. P. Zoombelt, S. G. J. Mathijssen, M. M. Wienk, M. Turbiez, D. M. de Leeuw and R. A. J. Janssen, *J. Am. Chem. Soc.*, 2009, **131**, 16616.
16 Y. Li, S. P. Singh and P. Sonar, *Adv. Mater.*, 2010, **22**, 4862–4866.
17 P. Sonar, S. P. Singh, Y. Li, M. S. Soh and A. Dodabalapur, *Adv. Mater.*, 2010, **22**, 5409–5411.
18 J. Lee, S. Cho and C. Yang, *J. Mater. Chem.*, 2011, **21**, 8528–8531.
19 Y. Li, P. Sonar, S. P. Singh, W. Zeng and M. S. Soh, *J. Mater. Chem.*, 2011, **21**, 10829–10835.
20 T. Lei, Y. Cao, Y. Fan, C. Liu, S. Yuan and J. Pei, *J. Am. Chem. Soc.*, 2011, **133**, 6099–6101.
21 I. Osaka, G. Sauvé, R. Zhang, T. Kowalewski and R. D. McCullough, *Adv. Mater.*, 2007, **19**, 4160–4165.
22 I. Osaka, R. Zhang, J. Liu, D. Smilgies, T. Kowalewski and R. D. McCullough, *Chem. Mater.*, 2010, **22**, 4191–4196.
23 H. A. Becerril, N. Miyaki, M. L. Tang, R. Mondal, Y. Sun, A. C. Mayer, J. E. Parmer, M. D. McGehee and Z. Bao, *J. Mater. Chem.*, 2009, **19**, 591–593.
24 R. Mondal, N. Miyaki, H. A. Becerril, J. E. Norton, J. Parmer, A. C. Mayer, M. L. Tang, J. Brédas, M. D. McGhee and Z. Bao, *Chem. Mater.*, 2009, **21**, 3618–3628.
25 H. Bronstein, Z. Chen, R. S. Ashraf, W. Zhang, J. Du, J. R. Durrant, P. S. Tuladhar, K. Song, S. E. Watkins, Y. Geerts, M. M. Wienk, R. A. J. Janssen, T. Anthopoulos, H. Sirringhaus, M. Heeney and I. McCulloch, *J. Am. Chem. Soc.*, 2011, **133**, 3272–3275.
26 X. Guo, F. S. Kim, S. A. Jenekhe and M. D. Watson, *J. Am. Chem. Soc.*, 2009, **131**, 7206–7207.
27 M. Yuan, M. Chiu, S. Liu, C. Chen and K. Wei, *Macromolecules*, 2010, **43**, 6936–6938.
28 J. A. Letizia, M. R. Salata, C. M. Tribout, A. Facchetti, M. A. Ratner and T. J. Marks, *J. Am. Chem. Soc.*, 2008, **130**, 9679–9694.
29 H. Meng and F. Wudl, *Macromolecules*, 2001, **34**, 1810–1816.
30 X. Guo, R. P. Ortiz, Y. Zheng, M. Kim, S. Zhang, Y. Hu, G. Lu, A. Facchetti and T. J. Marks, *J. Am. Chem. Soc.*, 2011, **133**, 13685–13697.
31 C. D. Dimitrakopoulos and P. R. L. Malenfant, *Adv. Mater.*, 2002, **14**, 99–117.
32 S. Kotani, K. Shiina and K. Sonogashira, *J. Organomet. Chem.*, 1992, **429**, 403.
33 J. A. Letizia, M. R. Salata, C. M. Tribout, A. Facchetti, M. A. Ratner and T. J. Marks, *J. Am. Chem. Soc.*, 2008, **130**, 9679.
34 X. Guo, M. D. Watson, F. S. Kim and S. A. Jenekhe, *J. Am. Chem. Soc.*, 2009, **131**, 7206.
35 C. Piliego, C. H. Woo, P. M. Beaujuge, J. M. J. Frechet, T. W. Holcombe and J. D. Douglas, *J. Am. Chem. Soc.*, 2010, **132**, 7595.
36 J. Lee, M. C. Gwinner, R. Berger, C. Newby, R. Zentel, R. H. Friend, H. Sirringhaus and C. K. Ober, *J. Am. Chem. Soc.*, 2011, **133**, 9949–9951.
37 J. L. Bredas, R. Silbey, D. S. Boudreaux and R. R. Chance, *J. Am. Chem. Soc.*, 1983, **105**, 6555–6559.
38 D. W. De Leeuw, M. M. J. Simenon, A. R. Brown and R. E. F. Einerhand, *Synth. Met.*, 1997, **87**, 53–59.
39 J. Pommerehne, H. Vestweber, W. Guss, R. F. Mahrt, H. Bssler, M. Porsch and J. Daub, *Adv. Mater.*, 1995, **7**, 551–554.
40 K. Eichkorn, O. Treutler, H. Öhm, M. Häser and R. Ahlrichs, *Chem. Phys. Lett.*, 1995, **242**, 652–660.
41 M. J. Frisch, G. W. Trucks, H. B. Schlegel, G. E. Scuseria, M. A. Robb, J. R. Cheeseman, G. Scalmani, V. Barone, B. Mennucci, G. A. Petersson, H. Nakatsuji, M. Caricato, X. Li, H. P. Hratchian, A. F. Izmaylov, J. Bloino, G. Zheng, J. L. Sonnenberg, M. Hada, M. Ehara, K. Toyota, R. Fukuda, J. Hasegawa, M. Ishida, T. Nakajima, Y. Honda, O. Kitao, H. Nakai, T. Vreven, J. A. Montgomery, J. E. Peralta, F. Ogliaro, M. Bearpark, J. J. Heyd, E. Brothers, K. N. Kudin, V. N. Staroverov, R. Kobayashi, J. Normand, K. Raghavachari, A. Rendell, J. C. Burant, S. S. Iyengar, J. Tomasi, M. Cossi, N. Rega, J. M. Millam, M. Klene, J. E. Knox, J. B. Cross, V. Bakken, C. Adamo, J. Jaramillo, R. Gomperts, R. E. Stratmann, O. Yazyev, A. J. Austin, R. Cammi, C. Pomelli, J. W. Ochterski, R. L. Martin, K. Morokuma, V. G. Zakrzewski, G. A. Voth, P. Salvador, J. J. Dannenberg, S. Dapprich, A. D. Daniels, O. Farkas, J. B. Foresman, J. V. Ortiz, J. Cioslowski, and D. J. Fox, *Gaussian 09, Revision A.02*, Gaussian, Inc., Wallingford, CT, 2009.

